

Photoproduction of axion-like particles at NA64

R. R. Dusaev^{*},¹ D. V. Kirpichnikov[†],² and M. M. Kirsanov[‡]²

¹*Tomsk State University, 634050 Tomsk, Russia*

²*Institute for Nuclear Research of the Russian Academy of Sciences, 117312 Moscow, Russia*

(Dated: July 17, 2022)

Axion-like particles a (ALPs) that couple to the Standard Model (SM) gauge fields could be observed in the high-energy photon scattering $\gamma N \rightarrow Na$ off nuclei followed by the $a \rightarrow \gamma\gamma$ decay. In the present paper we describe the calculation of the ALP production cross-section and its usage in the program for the simulation of events in the NA64 experiment, the active electron beam dump facility at the CERN SPS. Photons are produced in the electron bremsstrahlung in the target, they are simulated by the program based on the **GEANT4** package. The simulation of the a production and decays $a \rightarrow \gamma\gamma$ is implemented in the same program. We use this program to study the prospects of the NA64 experiment to search for ALP in the $10 \text{ MeV} \lesssim m_a \lesssim 100 \text{ MeV}$ mass range for the statistics corresponding to up to 5×10^{12} electrons on target.

I. INTRODUCTION

Axion-like particles interacting with gauge bosons of the Standard Model (SM) arise naturally in various well motivated SM extensions such as string theory [1, 2] and supersymmetry [3, 4]. Being a pseudo Nambu-Goldstone boson of spontaneously broken global Peccei-Quinn symmetry [5], ALP originally addressed the strong-CP problem [5–7]. More recently the interest to a new light and weakly coupled pseudo-scalar particle has been stimulated due to its relevance to the well motivated Dark Matter (DM) models [8, 9].

The aim of the present manuscript is to study the ALP production in the electron fixed target experiment through the Primakoff reaction $\gamma N \rightarrow Na$. The NA64 experiment is a sophisticated electron active beam dump facility with a significant potential to probe various scenarios beyond the Standard Model (BSM). The well-motivated dark sector of particle physics has been already constrained by NA64 using the missing energy signatures [10–13]. Moreover, the new experimental bounds on the ${}^8\text{Be}^*$ anomaly [14] have been derived by the NA64 experiment from the absence of displaced decays of hidden particle into electron-positron pairs [15, 16] in the decay volume of NA64.

Probing pseudo-scalar particles in the MeV to GeV mass range by the beam-dump facilities will be a hot experimental topic in the nearest future. For instance, such experiments as FASER [17], MATHUSLA [18], SHIP [19], CodexB [20], SeaQuest [21] and LDMX [22] will be able to probe long-lived ALP [23, 24] due to longer distances between ALP production point in a shield and downstream detectors. In these experiments ALP propagates typically along a distance of $10 - 100$ m before decay. This implies that the above-mentioned experimental facilities are sensitive to a relatively small cou-

plings in the range $10^{-7} \text{ GeV}^{-1} \lesssim g_{a\gamma\gamma} \lesssim 10^{-4} \text{ GeV}^{-1}$. On the other hand, the typical decay length in the NA64 experiment is several meters depending on the NA64 geometry setup. Therefore, due to this shorter length in this experiment it is possible to search for decays of ALP with $g_{a\gamma\gamma} \gtrsim 10^{-4} \text{ GeV}$ for sub-GeV m_a . In addition, it is possible to search for long-lived ALP in the missing energy signatures.

The paper is organised as follows. In Sec. II we discuss the properties of ALP. In Sec. III we review the ALP production cross-section in the Primakoff reaction. In Sec. IV we discuss the Monte-Carlo (MC) simulation of the ALP production in the NA64 experiment and estimate the sensitivity of this facility to the ALP for the statistics up to 5×10^{12} electrons on target.

II. THE ALP PROPERTIES

We consider the simplified setup [25] of ALP coupling predominantly to photons:

$$\mathcal{L}_{int} \supset -\frac{1}{4}g_{a\gamma\gamma}aF_{\mu\nu}\tilde{F}^{\mu\nu} + \frac{1}{2}(\partial_\mu a)^2 - \frac{1}{2}m_a^2a^2, \quad (1)$$

where $F_{\mu\nu}$ denotes the strength of the photon field, and the dual tensor is defined by $\tilde{F}_{\mu\nu} = \frac{1}{2}\epsilon_{\mu\nu\lambda\rho}F^{\lambda\rho}$. We assume throughout the paper that the effective coupling, $g_{a\gamma\gamma}$, and the ALP mass, m_a , are independent. The pseudoscalar boson coupled to photons (1) has the following decay width

$$\Gamma_{a \rightarrow \gamma\gamma} = \frac{g_{a\gamma\gamma}^2 m_a^3}{64\pi}. \quad (2)$$

The decay length of ALP is given by

$$l_a \simeq 4m \frac{E_a}{10^2 \text{ GeV}} \left(\frac{g_{a\gamma\gamma}}{10^{-4} \text{ GeV}^{-1}} \right)^{-2} \left(\frac{m_a}{10^2 \text{ MeV}} \right)^{-4}, \quad (3)$$

where E_a is the ALP energy. The minimal decay length to which the NA64 facility is sensitive is of the order of the target thickness (0.5m). Therefore, from Eq. (3) one

^{*}e-mail: renat.dusaev@cern.ch

[†]e-mail: kirpitch@ms2.inr.ac.ru

[‡]e-mail: mikhail.kirsanov@cern.ch

can conclude that NA64 with a most used beam energy of 100 GeV is sensitive to the values of ALP coupling to photons of the order of $g_{a\gamma\gamma} \gtrsim 10^{-4} \text{ GeV}^{-1}$.

III. CROSS-SECTION

We first calculate the cross-section of axions produced in the Primakoff process $\gamma N \rightarrow aN$. The ALP production amplitude is given by

$$\mathcal{M} = g_{a\gamma\gamma} e F(q^2) \epsilon_{\mu\nu\lambda\rho} \epsilon_i^\mu(p) p^\lambda q^\rho (\mathcal{P}_i + \mathcal{P}_f)^\nu \frac{1}{q^2}, \quad (4)$$

where $p, \mathcal{P}_i, \mathcal{P}_f$ and k are the four-momenta of the incident photon, initial nucleus, final state nucleus and the axion respectively, e is the electron charge. The internal photon momentum is defined by $q = \mathcal{P}_i - \mathcal{P}_f$. In Eq.(4) we suppose that the nucleus has spin zero, thus corresponding nuclear-photon vertex is given by [28–31]

$$ieF(q^2)(\mathcal{P}_i + \mathcal{P}_f).$$

The form-factor $F(q^2)$ depends upon the value of momentum transfer $q^2 = -t$ and describes the elastic photon scattering

$$F(t) \approx Z \left(\frac{a^2 t}{1 + a^2 t} \right) \left(\frac{1}{1 + t/d} \right), \quad (5)$$

where $a = 111Z^{-1/3}/m_e$ and $d = 0.164 \text{ GeV}^2 A^{-2/3}$, here m_e is the mass of electron and A is the atomic weight. The inelastic form-factor proportional to \sqrt{Z} is small as compared to (5) for the high- Z target material and thus yields a subdominant contribution to the signal process. The differential cross-section of the elastic processes $\gamma N \rightarrow Na$ in the lab frame is given by

$$d\sigma = \frac{1}{2^5 \pi} \frac{1}{E_\gamma^2 M_N} \overline{|\mathcal{M}|^2} dE_a, \quad (6)$$

where E_γ is the incoming photon energy and M_N is the mass of nucleus. The amplitude squared (see, e. g. Eq. (4) for details) averaged over the initial photon polarizations is given by

$$\begin{aligned} \overline{|\mathcal{M}|^2} &= \frac{1}{2} \sum_{pol.} |\mathcal{M}|^2 = g_{a\gamma\gamma}^2 e^2 F^2(q) M_N^2 \frac{1}{2t^2} \times \\ &\left[(4E_a^2 t - (m_a^2 + t)^2) - \frac{2E_a t (m_a^2 - t)}{M_N} - \frac{m_a^2 t^2}{M_N^2} \right] \end{aligned} \quad (7)$$

here we use the `FeynCalc` package [32] of `Wolfram Mathematica` [33] that carries out a summation in $\overline{|\mathcal{M}|^2}$ over dump indices. The resulting amplitude squared is given by

$$\overline{|\mathcal{M}|^2} \simeq g_{a\gamma\gamma}^2 e^2 F^2(t) M_N^2 \times \frac{1}{2t^2} (4E_a^2 t - m_a^4),$$

where we suppose that $m_a \gg t$ and neglect the third and fourth terms of Eq. (7) since the target nuclei are rather heavy, $M_N \gg m_a$ and $M_N \gg \sqrt{t}$. The angle θ_a between the incoming photon and ALP can be derived from the momentum conservation law. The latter implies the following expression

$$\cos \theta_a = \frac{1}{2|\mathbf{p}_a|E_\gamma} \cdot (2E_a(E_\gamma + M_N) - 2E_\gamma M_N - m_a^2). \quad (8)$$

For NA64 experiment we are mainly interested in high energy photons produced by 100 GeV electrons in the lead target. This corresponds to small momentum transfers and to small angles of ALP emission. In particular, we consider the limit when $m_a \ll E_a$ and $\theta_a \ll 1$, then Eq. (8) implies that the photon energy can be expressed as

$$E_\gamma \approx E_a + \frac{E_a^2 \theta_a^2}{2M_N} + \frac{m_a^4}{8M_N E_a^2}. \quad (9)$$

In this approach the ALP energy can be rewritten as follows

$$E_a \approx E_\gamma - \frac{E_\gamma^2 \theta_a^2}{2M_N} - \frac{m_a^4}{8M_N E_\gamma^2}. \quad (10)$$

We note that one should not neglect the last term in Eq. (10) which is naively associated with a typical angle of ALP emission. In particular, from Eq. (10) follows that the momentum transfer squared can be approximated as

$$t = -q^2 = 2M_N(E_\gamma - E_a) \approx E_\gamma^2 \theta_a^2 + \frac{1}{4} \frac{m_a^4}{E_\gamma^2}. \quad (11)$$

It is worth mentioning, however, that realistic typical angle of ALP production depends also on the properties of atomic form-factors (see, e. g. Eq. (17) below for details). Finally, one can obtain the momentum transfer distribution from Eqs. (6) and (11)

$$\frac{d\sigma}{dt} = \frac{1}{2^3} \cdot g_{a\gamma\gamma}^2 \alpha F^2(t) \cdot \frac{1}{t^2} (t - t_{min}) \quad (12)$$

where $t_{min} = m_a^4/(4E_\gamma^2)$. The differential cross-section $d\sigma/dt$ has a peak at

$$t^* = 2t_{min} + 1/a^2, \quad (13)$$

which is associated with typical momentum transfers. In the left panel of Fig. 1 we show $d\sigma/dt$ as a function of t for various masses m_a and typical energies of incoming photons E_γ . We note that the maximum allowed value of momentum transfer is given by

$$q_{max} = \sqrt{t_{max}} = \sqrt{2M_N(E_\gamma - m_a)}.$$

For the typical threshold energy of interest $E_\gamma > 50 \text{ GeV}$ we have $q_{max} \gg \sqrt{t_{min}}$. From the left panel of Fig. 1 it is seen that the cross-section of ALP production is highly

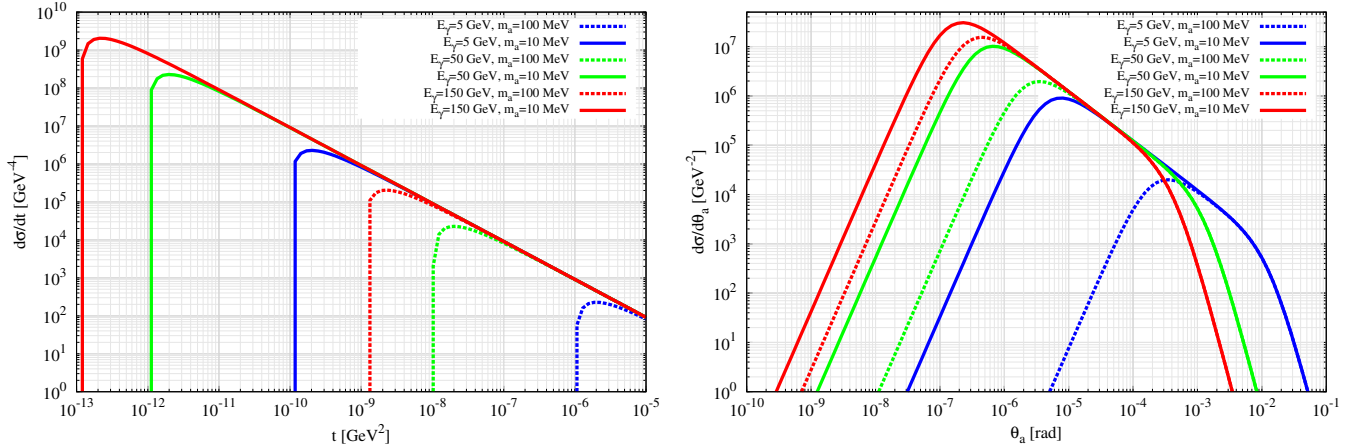


FIG. 1: Left: differential cross-section versus momentum tranfer squared. Right: differential cross-section versus angle of ALP emission. All cross-sections are calculated for lead target and $g_{a\gamma\gamma} = 1 \text{ GeV}^{-1}$.

suppressed in the region of this value. This means that one can set $t_{max} = \infty$ in the integration of Eq. (12) over t . Thus the total cross-section of the Primakoff process is

$$\sigma_{tot} = \frac{1}{2^3} g_{a\gamma\gamma}^2 \alpha \int_{t_{min}}^{\infty} \frac{dt}{t^2} (t - t_{min}) F^2(t). \quad (14)$$

For the typical wide range of ALP masses, $20 \text{ MeV} \lesssim m_a \lesssim 100 \text{ MeV}$ and typical energies of photons, $50 \text{ GeV} \lesssim E_\gamma \lesssim 100 \text{ GeV}$, the parameters of lead form-factors ($Z = 82$ and $A = 207$) satisfy $d \gg t_{min}$ and $d \gg 1/a^2$. Given that approach, one has the following expression for the total cross-section in the leading logarithmic order

$$\sigma_{tot} = \frac{16\pi\alpha}{m_a^3} \cdot \Gamma_{a \rightarrow \gamma\gamma} \cdot \frac{Z^2}{2} \left(\ln \left[\frac{d}{1/a^2 + t_{min}} \right] - 2 \right). \quad (15)$$

The total cross-section depends rather weakly on m_a and E_γ , see Fig. 2.

From Eqs. (6), (7), (10) and (11) we obtain

$$d\sigma \approx \frac{1}{m_a^3} 16\pi\alpha F^2(t) \Gamma_{a \rightarrow \gamma\gamma} \frac{\theta_a^3 d\theta_a}{(\theta_a^2 + \delta_a^2)^2}, \quad (16)$$

where $\delta_a \approx m_a^2/(2E_\gamma^2)$ is a parameter that characterizes a typical angle between the beam line and the ALP momentum. This result coincides with [25–27]. We note that $d\sigma/d\theta_a$ has a peak at

$$\theta_a^* \approx \frac{1}{aE_\gamma} \sqrt{3(1 + a^2 t_{min})}, \quad (17)$$

This is a typical angle of ALP, see the right panel of Fig. 1. For $a^2 t_{min} \gg 1$ it is proportional to δ_a , and for $a^2 t_{min} \ll 1$ it is scaled as $\propto 1/(aE_\gamma)$.

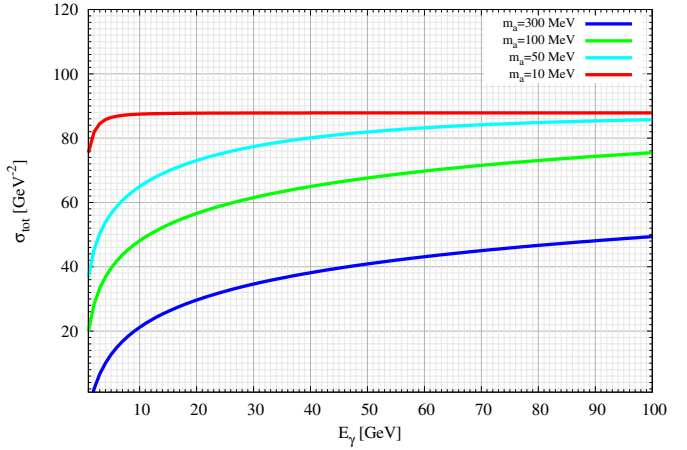


FIG. 2: Total cross-section versus incident photon energy for lead target and $g_{a\gamma\gamma} = 1 \text{ GeV}^{-1}$.

IV. CALCULATION OF THE ALP YIELD IN NA64

In this section we discuss the implementation of the code for the MC simulation of the ALP production that uses the formulas derived above in the full simulation program based on **GEANT4** [35] for the NA64 experiment [12]. The photons that can produce ALP originate from the bremsstrahlung radiation of electrons and positrons of the electromagnetic shower from the primary 100 GeV electron beam absorbed in the target - calorimeter ECAL. The Primakoff process of ALP production $\gamma N \rightarrow aN$ in this program can occur along with other, SM processes, for all photons of the electromagnetic shower if the photon energy E_γ is above some threshold that corresponds to the minimal detectable ALP energy.

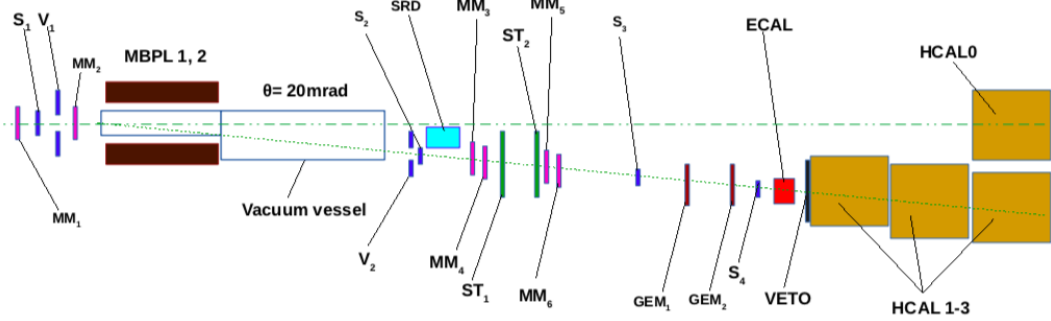


FIG. 3: The NA64 configuration for the search for invisible dark photons decays (invisible mode geometry)

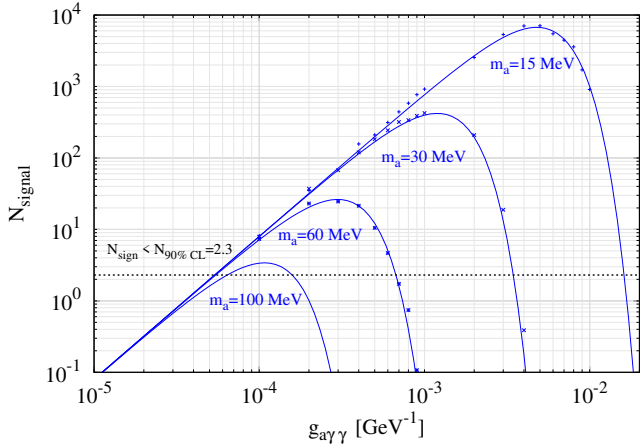
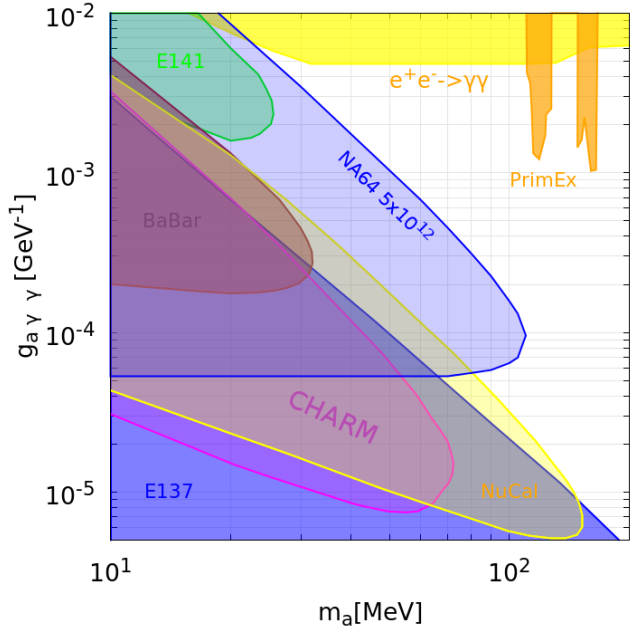


FIG. 4: Number of signal events as a function of $g_{a\gamma\gamma}$ for invisible mode setup and for $N_{EOT} = 5 \times 10^{12}$ with 100% efficiency.



After production the ALP decay is simulated according to Eq.(2). In order to simulate sufficient number of samples with sufficient statistics we used the CERN batch system. This production process was automatized [34]. We assumed the configuration of NA64 designed for the search of invisible decays of dark photons A' , see Fig. 3. In this configuration the target - calorimeter ECAL is followed by three modules of the hadron calorimeter HCAL. We assume that ALPs decay predominantly to photons $\mathcal{B}(a \rightarrow \gamma\gamma) \approx 1$. In the present paper we consider the following scheme of ALP probing.

Two distinct signatures of ALP in the NA64 experiment are possible. In the first signature the ALP decays in the second and third modules of HCAL, the first module (HCAL1) serving as a veto. In the second signature the ALP decays beyond all subdetectors of NA64. This is the missing energy signature of ALP, the same that is described in [10–13]. In the second (missing energy) signature the cut on the ECAL energy is rather strict,

FIG. 5: The expected 90 % C.L. sensitivity region of NA64 to the ALP production in the Primakoff process, $\gamma N \rightarrow aN$ followed by the decay into photon pairs $a \rightarrow \gamma\gamma$ (light blue region). The limits for E137 [26], CHARM [36], NuCal [37], BaBar [38], E141 [39], LEP [40] ($e^+e^- \rightarrow \gamma\gamma$) and PrimEx [41] are taken from Refs. [42, 43].

$E_{ECAL} < 50$ GeV. This means that only shower photons with the energy above 50 GeV can produce detectable ALP. The background conditions in the first signature are much better, for this reason it is possible to relax the cut on E_{ECAL} . It is defined by the trigger and is about 80 GeV. Correspondingly, in this signature photons with the energy as low as $\simeq 20$ GeV can produce detectable ALP. The flux of such photons is significantly higher. In the signal samples we simulated the ALP with the energy $E_{ALP} > 18$ GeV decaying beyond the HCAL1 module,

which includes also $a \rightarrow \gamma\gamma$ decays far from the NA64 detectors. The cuts corresponding to the two signatures were applied during the processing of these samples by the reconstruction program.

Now we describe the calculation of the ALP signal in NA64 at each step of the photon propagation in the target. The number of ALP produced at the i -th photon's step in the electromagnetic shower is

$$N_a^{(i)} = \frac{\rho N_A}{A} \sigma_{tot}(E_\gamma^i) \times l_i \quad (18)$$

where ρ is a density of the lead ECAL active target, A is the atomic mass of the target, N_A is Avogadro's number, $\sigma_{tot}(E_\gamma^i)$ is the total cross-section of ALP elastic interaction with a nucleus (see, e. g. Eq. (15) for details), l_i is the step length.

In the **GEANT4** simulation of signal samples, at each step of tracing of a photon with the energy above threshold the following actions are made

- first we randomly sample the variable u distributed uniformly in the range $[0, 1]$, if u is smaller than the a emission probability

$$P_{emission} = \frac{\rho N_A}{A} \times \sigma_{tot}(E_\gamma^i) \times l_i$$

then the emission of a is accepted,

- for each emitted a we then generate the value of E_a/E_γ and the angle of a w.r.t. the initial photon according to the differential cross section (Fig. 1), then we calculate the four-momentum of ALP. The value of E_a/E_γ is very close to unity, $E_a/E_\gamma \simeq 1$.

Now we estimate the sensitivity of NA64 to ALPs. The number of detectable ALPs can be written as

$$N_a = \frac{N_{EOT}}{N_{MC}} \sum_i N_a^{(i)} \exp\left(-L_D^{(i)}/l_a^{(i)}\right) \mathcal{B}(a \rightarrow \gamma\gamma), \quad (19)$$

where N_{EOT} is the number of electrons on target in the experiment, N_{MC} is the number of simulated events, $L_D^{(i)}$ is the distance from the production point to the minimal allowed Z coordinate Z_{min} , $l^{(i)}$ is the ALP decay length taking into account its gamma factor. Z_{min} can be the end of HCAL1 or the end of HCAL3 depending on the signature that we study. The typical lengths here are the lengths of the calorimeters $L_{ECAL}=45\text{cm}$ and $L_{HCAL\ module}=1.3\text{m}$. The typical energy of ALP in the Primakoff process is $E_a \approx E_\gamma$, therefore the ALP spectra

are associated with the spectra of shower photons in the dump.

In Fig. 4 we show the number of $a \rightarrow \gamma\gamma$ decays as a function of ALP coupling with photons. Assuming background free case and zero signal events observed at NA64 we require 90% CL upper limit on number of ALP decays to be $N_{90\%} = 2.3$ according to Poisson statistics. For each ALP mass m_a the range of couplings constrained $g_{a\gamma\gamma}^{low}(m_a) < g_{a\gamma\gamma} < g_{a\gamma\gamma}^{up}(m_a)$ is defined by inequality $N_a > N_{90\%}$, see Fig. 4. The values above $g_{a\gamma\gamma}^{up}$ correspond to short-lived ALP that decay too quickly to detect them. The values below $g_{a\gamma\gamma}^{low}$ correspond to too small signal yield. The resulting plot in Fig. 4 includes both visible and invisible signatures.

In Fig. 5 we show the 90% C.L. sensitivity region of the invisible mode setup of NA64 in the ALP parameters space for the background free case and the total number of 100 GeV electrons on target $N_{EOT} = 5 \times 10^{12}$ in the mass range $10\text{ MeV} \lesssim m_a \lesssim 100\text{ MeV}$. The detector efficiency is assumed to be 100%. These results show that the NA64 experiment potentially allows to probe the ALP coupling with photons in the range $5 \times 10^{-5}\text{ GeV}^{-1} \lesssim g_{a\gamma\gamma} \lesssim 10^{-3}\text{ GeV}^{-1}$.

V. CONCLUSION

In the present manuscript we have studied the prospects of NA64 to search for ALP in the fixed target experiment on the electron beam at the CERN SPS. In particular, we have studied the detection signatures of ALPs produced in the Primakoff reaction $\gamma N \rightarrow Na$ in the active target of NA64 followed by the ALP decay $a \rightarrow \gamma\gamma$. We have implemented the ALP production cross-sections in the **GEANT4** based simulation program for NA64. We have calculated the expected sensitivity to ALP of the NA64 experiment and have shown that it can allow to examine the unexplored region in the parameter space $5 \times 10^{-5}\text{ GeV}^{-1} \lesssim g_{a\gamma\gamma} \lesssim 10^{-3}\text{ GeV}^{-1}$ and $10\text{ MeV} \lesssim m_a \lesssim 100\text{ MeV}$ if the statistics corresponding to $N_{EOT} = 5 \times 10^{12}$ electrons on target is accumulated.

VI. ACKNOWLEDGEMENTS

We would like to thank our colleagues from the NA64 Collaboration, in particular, S. N. Glinenko, N. V. Krasnikov, P. Crivelli, D. S. Gorbulov and V. E. Lyubovitskij for useful discussions.

[1] P. Svrcek and E. Witten, JHEP **0606** (2006) 051 [hep-th/0605206].
[2] A. Arvanitaki, S. Dimopoulos, S. Dubovsky, N. Kaloper and J. March-Russell, Phys. Rev. D **81** (2010) 123530 [arXiv:0905.4720 [hep-th]].
[3] A. E. Nelson and N. Seiberg, Nucl. Phys. B **416** (1994) 46 [hep-ph/9309299].
[4] J. Bagger, E. Poppitz and L. Randall, Nucl. Phys. B **426** (1994) 3 [hep-ph/9405345].
[5] R. D. Peccei and H. R. Quinn, Phys. Rev. Lett. **38** (1977)

1440.

[6] S. Weinberg, Phys. Rev. Lett. **40** (1978) 223.

[7] F. Wilczek, Phys. Rev. Lett. **40** (1978) 279.

[8] C. Boehm and P. Fayet, Nucl. Phys. B **683** (2004) 219 doi:10.1016/j.nuclphysb.2004.01.015 [hep-ph/0305261].

[9] M. J. Dolan, F. Kahlhoefer, C. McCabe and K. Schmidt-Hoberg, JHEP **1503** (2015) 171 Erratum: [JHEP **1507** (2015) 103] [arXiv:1412.5174 [hep-ph]].

[10] S. N. Gninenko, N. V. Krasnikov, M. M. Kirsanov and D. V. Kirpichnikov, Phys. Rev. D **94** (2016) no.9, 095025 [arXiv:1604.08432 [hep-ph]].

[11] D. Banerjee *et al.* [NA64 Collaboration], Phys. Rev. Lett. **118** (2017) no.1, 011802 [arXiv:1610.02988 [hep-ex]].

[12] S. N. Gninenko, D. V. Kirpichnikov, M. M. Kirsanov and N. V. Krasnikov, Phys. Lett. B **782** (2018) 406 [arXiv:1712.05706 [hep-ph]].

[13] S. N. Gninenko, D. V. Kirpichnikov and N. V. Krasnikov, Phys. Rev. D **100** (2019) no.3, 035003 [arXiv:1810.06856 [hep-ph]].

[14] A. J. Krasznahorkay *et al.*, Phys. Rev. Lett. **116** (2016) no.4, 042501 [arXiv:1504.01527 [nucl-ex]].

[15] D. Banerjee *et al.* [NA64 Collaboration], Phys. Rev. Lett. **120** (2018) no.23, 231802 [arXiv:1803.07748 [hep-ex]].

[16] D. Banerjee *et al.* [NA64 Collaboration], arXiv:1912.11389 [hep-ex].

[17] A. Ariga *et al.* [FASER Collaboration], Phys. Rev. D **99** (2019) no.9, 095011 [arXiv:1811.12522 [hep-ph]].

[18] J. P. Chou, D. Curtin and H. J. Lubatti, Phys. Lett. B **767** (2017) 29 [arXiv:1606.06298 [hep-ph]].

[19] M. Anelli *et al.* [SHiP Collaboration], arXiv:1504.04956 [physics.ins-det].

[20] V. V. Gligorov, S. Knapen, M. Papucci and D. J. Robinson, Phys. Rev. D **97** (2018) no.1, 015023 [arXiv:1708.09395 [hep-ph]].

[21] A. Berlin, S. Gori, P. Schuster and N. Toro, Phys. Rev. D **98** (2018) no.3, 035011 [arXiv:1804.00661 [hep-ph]].

[22] T. Akesson *et al.* [LDMX Collaboration], arXiv:1808.05219 [hep-ex].

[23] J. Beacham *et al.*, J. Phys. G **47** (2020) no.1, 010501 [arXiv:1901.09966 [hep-ex]].

[24] R. Alemany *et al.*, arXiv:1902.00260 [hep-ex].

[25] B. Dobrich, J. Jaeckel, F. Kahlhoefer, A. Ringwald and K. Schmidt-Hoberg, JHEP **1602** (2016) 018, [arXiv:1512.03069 [hep-ph]].

[26] J. D. Bjorken *et al.*, Phys. Rev. D **38** (1988) 3375.

[27] Y. S. Tsai, Phys. Rev. D **34** (1986) 1326.

[28] Y. S. Liu and G. A. Miller, Phys. Rev. D **96** (2017) no.1, 016004 [arXiv:1705.01633 [hep-ph]].

[29] Y. S. Liu, D. McKeen and G. A. Miller, Phys. Rev. D **95** (2017) no.3, 036010 [arXiv:1609.06781 [hep-ph]].

[30] T. Beranek and M. Vanderhaeghen, Phys. Rev. D **89** (2014) no.5, 055006 [arXiv:1311.5104 [hep-ph]].

[31] T. Beranek, H. Merkel and M. Vanderhaeghen, Phys. Rev. D **88** (2013) 015032 [arXiv:1303.2540 [hep-ph]].

[32] V. Shtabovenko, R. Mertig and F. Orellana, Comput. Phys. Commun. **207** (2016) 432 [arXiv:1601.01167 [hep-ph]].

[33] Wolfram Research, Inc., Mathematica, Version 12.1, Champaign, IL (2020), <https://www.wolfram.com/mathematica>

[34] <https://gitlab.cern.ch/P348/na64-tools/tree/alps/geant4/simulation/examples/example100500>

[35] S. Agostinelli *et al.* [GEANT4 Collaboration], Nucl. Instrum. Meth. A **506** (2003) 250.

[36] F. Bergsma *et al.*, [CHARM Collaboration], Phys. Lett. B **157**, 458 (1985).

[37] J. Blümlein *et al.*, Z. Phys. C **51**, 341 (1991).

[38] B. Aubert *et al.* [BaBar Collaboration], arXiv:0808.0017 [hep-ex].

[39] M. W. Krasny *et al.* [E141 Collaboration], Preprint Univ. of Rochester, UR-1029 (1987);

[40] G. Abbiendi *et al.* [OPAL Collaboration], Eur. Phys. J. C **26**, 331 (2003).

[41] D. Aloni, C. Fanelli, Y. Soreq, M. Williams, Phys. Rev. Lett. **123**, 071801 (2019).

[42] M. J. Dolan, T. Ferber, C. Hearty, F. Kahlhoefer and K. Schmidt-Hoberg, JHEP **1712** (2017) 094 [arXiv:1709.00009 [hep-ph]].

[43] B. Dobrich, J. Jaeckel and T. Spadaro, JHEP **1905** (2019) 213 [arXiv:1904.02091 [hep-ph]].